Available online at www.sciencedirect.com
ScienceDirect
Focus Article, *Mendeleev Commun.*, 2009, **19**, 117–122
Mendeleev Communications

Extra-strong wear-resistant materials based on nanostructured crystals of partially stabilized zirconium dioxide

Vjacheslav V. Osiko

Laser Materials and Technology Research Center, A. M. Prokhorov General Physics Institute, Russian Academy of Sciences, 119991 Moscow, Russian Federation.
Fax: +7 499 135 7744; e-mail: osiko@lst.gpi.ru

DOI: 10.1016/j.mencom.2009.05.001

The preparation, properties and applications of nanostructured materials, namely, crystals of partially stabilized zirconium dioxide (PSZ), are summarised. PSZ is formed due to the self-organization of the nanostructure during the cubic-to-tetragonal phase transformation of single crystals, and as a result the bulk of the material is built of densely and orderly packed domains with characteristic sizes of 10–20 nm. Unique mechanical and physicochemical properties of PSZ crystals, such as extremely high impact strength and wear resistance combined with low friction factor, thermal stability, bioinertness, and biocompatibility, make them very attractive for many technical and medical applications.

Ceramics and single crystals based on solid solutions with zirconium dioxide as the main component, have been used as structural and functional materials for a few decades. The distinctive features of these materials include an outstanding physicochemical stability (especially at high temperatures and under oxidizing conditions), good structural and tribological properties, biocompatibility and bioinertness.[1] Recently, the elements of nanotechnology were introduced into the technologies of this class of materials and provided a considerable improvement in their specifications. It is well known that the modern technology of oxide ceramic materials involves a sequence of process steps, including the preparation of the starting nanopowders with preset chemical compositions, their classification, and preliminary compacting followed by sintering. Sintering occurs either under pressure that stimulates the compacting process or without pressure, where the decisive role belongs to the thermally stimulated self-assembly of nanoparticles into a polycrystalline product with a maximum density. Advances achieved in this field are well illustrated by the technology for the preparation of optically homogeneous laser ceramics from an yttrium–aluminium garnet combined with yttrium and scandium oxides developed by Japanese researchers.[2]

Recently, the technology of optical laser ceramics was also successfully implemented for fluorides.[3]

Another way to obtain structured nonmetallic materials is 'from top to bottom'. In the latter case, the role of raw materials is played by single crystals or compact polycrystalline ingots obtained by crystallization of melts. Then, upon applying an uniaxial mechanical stress or a more complex stress, such as pressure combined with torsion, to a preheated sample, the latter undergoes polygonization, which induces the formation of a micro- or nanocrystalline structure in the sample. This approach is widely used in metallurgy for modifying the mechanical properties of metals. As concerns dielectric materials, a recent example is provided by the preparation of nanostructured fluoride laser materials by thermomechanical deformation of the single crystals of corresponding fluorides.[3,4]

This paper describes a new method for the preparation of nanostructured oxide-based structural and functional materials – the method of nanostructure self-assembly during phase transformations in single crystals. Unlike the former two methods, this is not a general method since it cannot be applied with equal success to materials with different compositions. Nanostructured crystals of partially stabilized zirconium dioxide considered in this paper are likely to provide the first and, maybe, unique example of such a conversion among oxide materials, in contrast with metal systems where such conversions are quite common.[5] To clarify the essence of the processes that occur in zirconium dioxide-based solid solutions, let us remind the currently known data on phase transformations of zirconium dioxide and its solid solutions and the structure of corresponding phases.

Phase transformations and structure of zirconium dioxide-based solid solutions. Pure zirconium dioxide exists in three modifications: monoclinic (m), tetragonal (t) and cubic (c). The low-temperature monoclinic modification is stable up to 1160 °C. The tetragonal modification is stable in the range from 1160 to 2370 °C. From 2370 °C and up to the melting point (2680 °C), the cubic modification is stable.[6]

Vjacheslav V. Osiko is Academician of the Russian Academy of Sciences (RAS), professor, head of the Laser Materials and Technology Research Center at A. M. Prokhorov General Physics Institute of the RAS. His interests include laser physics and laser technologies and technologies of materials for photonics, including nanotechnologies. V. V. Osiko is the author of over 500 scientific works, inventions and books. He was awarded a Lenin prize in science and technology for the creation of new technologies of highly-refractory crystalline materials, Award of USSR Council of Ministers, E. S. Fedorov Award of the RAS, and Robert A. Laudise Prize of the International Organization for Crystal Growth.

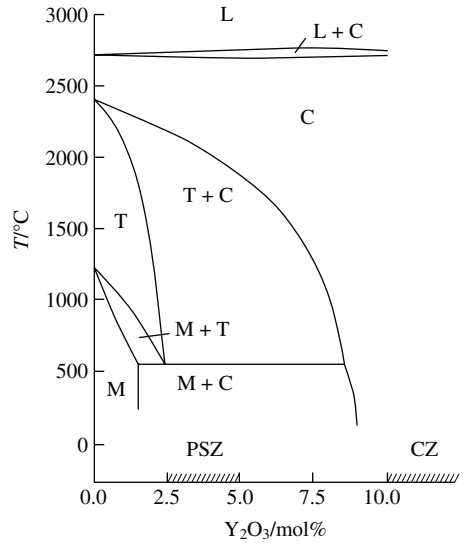

Figure 1 Part of the phase diagram for the ZrO_2–Y_2O_3 binary system (range of compositions adjacent to ZrO_2).[7] L – melt; phases: C – cubic, T – tetragonal, M – monoclinic. CZ – range of phianite compositions; PSZ – range of PSZ compositions.

The cubic phase of ZrO_2 has a non-distorted fluorite-type structure. Space group *Fm*3*m*.

The tetragonal modification of ZrO_2 has a slightly distorted fluorite structure (space group $P4_2/nmc$) with the following unit cell parameters: $a = b = 5.085$ Å, $c = 5.166$ Å, $a/c = 1.016$. Due to small shifts, the oxygen ions become displaced with respect to the ideal positions (1/4, 1/4, 1/4) typical of the fluorite lattice, so the original cube becomes slightly elongated along the *c* axis.

The structure of the *monoclinic modification* of ZrO_2 is characterized by space group $P2_1/c$ with the following parameters: $a = 5.169$ Å, $b = 5.232$ Å, $c = 5.341$ Å; $\beta = 99.15°$.[1] The crystals of this ZrO_2 modification occur in the Earth crust as the baddeleyite mineral. Its structure results from a further distortion of the cubic structure, which is reorganized to such an extent that a structure of a principally new type appears.

The trend of zirconium (and hafnium) dioxide to form solid solutions with Group II and III element oxides, such as MgO, CaO, SrO, Sc_2O_3, Y_2O_3 and Ln_2O_3 (where Ln means a rare-earth element), is well known. It is important that the formation of solid solutions considerably decreases the temperatures of both ZrO_2 phase transformations. In turn, this opens a way for kinetic stabilization of the high-temperature cubic modification of ZrO_2. The crystallochemical aspect of stabilization consists in the formation of a large number of anionic vacancies upon the formation of solid solutions. In fact, if the second component is a Group II element oxide (MgO, CaO or SrO), each formula unit of the oxide creates one vacancy, while for a sesquioxide, one vacancy is created by every two $MO_{1.5}$ formula units. Figure 1 shows a part of the diagram for the ZrO_2–Y_2O_3 binary system.[7] Note that, in comparison with the diagrams published by other authors, the diagram presented here is most completely confirmed by current experimental data. One can see from the drawing that, in the range of ZrO_2-rich compositions, broad regions of solid solutions of all three structural types characteristic of ZrO_2 are formed, namely, cubic, tetragonal and monoclinic. This fact is widely used in the production of ZrO_2-based ceramic materials obtained by sintering, including the sintering of nanopowders.

In a number of papers,[1,6,8–13] we have substantiated and elaborated a method for synthesizing single-crystal refractory oxide materials, including ZrO_2-based solid solutions, by crystallization of appropriate melts.

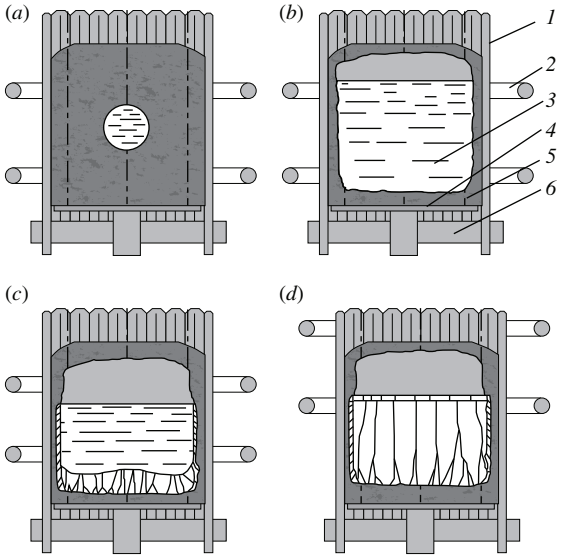

Figure 2 Stages of the synthesis of PSZ crystals by directed crystallization of a melt in a cold crucible with the use of direct RF-heating: (*a*) initial melting, (*b*) melt buildup stage and melt homogenization, (*c*) crystal growth stage and (*d*) complete crystallization of the melt bulk and controlled nanostructuring. (*1*) cold crucible walls, (*2*) RF coil, (*3*) melt, (4) cooled bottom, (*5*) skull and (*6*) isolating ring.

Synthesis of zirconium dioxide-based solid solution crystals from a melt. Phianites, C-OX and PSZ. The physical base of the developed technology of highly refractory materials involves the melting and subsequent crystallization of melts in a cold crucible by direct induction heating of the melt.[1] In this case, the melt is enclosed in a solid polycrystalline shell with a chemical composition identical to that of the melt. This method and the corresponding technologies are currently widespread both in Russia and worldwide. The most advanced product of these technologies is phianite crystals that are ZrO_2 (or HfO_2) based solid solutions with a cubic structure. Figure 2 demonstrates the main stages in the preparation of crystals of phianites and other ZrO_2-based materials.[1,14]

Several types of high-performance production equipment have been developed and are being manufactured in the Russian Federation: Crystal-401, Crystal-403, Crystal-405 (Table 1). Moreover, the Phianite-700 unit with a cold crucible diameter of 700 mm has been created. Table 2 lists the main parameters of this unit.

Table 1 Technical specifications of setups for direct high-frequency melting of dielectrics in a cold crucible.

Parameter	Setup specifications		
	Crystal-401	Crystal-403	Crystal-405
Input power/kW	100	280	280
Oscillating power/kW	60	160	160
Current frequency/MHz	5.28	1.76	1.76
Crucible inner diameter/mm	200	400	500
Crucible height/mm	300	700	1000
Working temperature of the melt/K	3000	2900	2900
Productivity/kg h^{-1}: phianites, fused oxides	0.15	3.0 25	3.0

Table 2 Main technical specifications of experimental setup 'Phianite-700'.

Specification	Value
Cold crucible inner diameter/mm	700
Consumed power/kW	600
Current frequency/kHz	400–800
Inductor motion rate/mm h^{-1}	2–30
Mass of crystallized melt/kg	600–1000
Mass of individual crystals/kg	up to 10

Figure 3 Crystals of phianites, C-OX and PSZ and some articles made thereof.

Let us once again remind you the main advantages of the newly developed technologies:

– versatility; feasibility of melting and crystallizing dielectric materials with any melting points and diverse chemical compositions;

– high chemical purity of the process; absence of contact with chemically-foreign materials;

– high economical efficiency; up to 600–700 kg of the crystalline material can be produced in one technological cycle; the absence of special requirements for the granulometric composition of the original stock;

– there is almost no waste as the crystalline waste can be recycled.

Depending on the type of the stabilizing oxide and its concentration, and by combining two or more such oxides, the above method allows one to prepare various crystalline products (Table 3).

The concentration ranges of the stabilizing oxide corresponding to the formation of phianite and PSZ crystals are shown in Figure 1 (phase diagram). Figure 3 shows pictures of some crystals of phianites, C-OX and PSZ.

Formation and structure of PSZ crystals. Ceramics based on partially stabilized zirconium dioxide are well known and have been used in practice for a long time. In 1981, Raman scattering studies of ZrO_2–Gd_2O_3 (8 mol%) and ZrO_2–Eu_2O_3 (8 mol%) single crystals obtained by crystallization of melts showed for the first time that, unlike phianites with other compositions, which invariably have a cubic fluorite-type structure, these crystals had a tetragonal structure and were built of densely and orderly packed domains, whereas the continuity and optical homogeneity of the crystals were retained.[15,16] Detailed studies of crystalline solid solutions based on ZrO_2 (HfO_2) with concentrations of stabilizing oxides from 2 to 6 mol% allowed us to create a series of PSZ crystals. The current concept about the mechanism of formation of PSZ crystals is as follows.

Table 3 Crystalline materials based on ZrO_2-based solid solutions.

Crystal type	Type of the stabilizing oxide	Concentration of the stabilizing oxide	Structure
Phianites	Y_2O_3, Eu_2O_3, Gd_2O_3, Dy_2O_3, Er_2O_3, Tm_2O_3, Y_2O_3, Ho_2O_3, Yb_2O_3, Lu_2O_3, CaO	10–20 mol% (Y_2O_3)	Cubic, fluorite (single crystal)
C-OX (cubic oxide) crystals	$Y_2O_3 + Ce_2O_3$, $Y_2O_3 + Pr_2O_3$, $Y_2O_3 + Nd_2O_3$, $Y_2O_3 + Co_2O_3$	20–30 mol% (Y_2O_3, Yb_2O_3, Lu_2O_3), 5 mol% (Ce_2O_3, Pr_2O_3, Nd_2O_3)	Cubic, tetrahedral coordination of impurity ions in single crystals
PSZ	Y_2O_3, Gd_2O_3 and other rare-earth metal oxides, CaO	2.5–5 mol% Y_2O_3	Coherent nanostructured crystals, tetragonal

Directed crystallization of melts with the composition ZrO_2–2–6 mol% Y_2O_3 gives crystals of the cubic modification in accordance with the state diagram (Figure 1). As the temperature front advances and the crystals that have grown are gradually cooled to the temperature of cubic-to-tetragonal transition (2400–2300 °C depending on the concentration of the stabilizer oxide), the crystals remain cubic and retain phase uniformity. On subsequent slow cooling, the cubic structure is transformed to a tetragonal structure. This structure is preserved on cooling to room temperature. The resulting crystals (Figure 3) visually do not differ from phianite crystals in size, shape and surface smoothness. However, unlike phianites, they are milk-white, which is an external evidence of the phase transformation that occurred in them. It is remarkable that (1) the crystals remain continuous and contain no cracks; (2) there is no visual evidence of volume changes due to the phase transformation; separate crystals in a block of grown crystals are as densely packed in the bulk of the ingot as in the case of phianites: there are no gaps between the crystals. For comparison: upon crystallization of a melt of pure ZrO_2 due to cubic → tetragonal → monoclinic phase transformations, a polycrystalline bulk with numerous cracks is formed, which implies a considerable decrease in volume during structural transformations.

Numerous studies on the mechanism of structural transformations during the formation of PSZ crystals have been published; the conclusions made are often contradictory, which implies the complexity of these processes (*e.g.,* see refs. 17–22). Structural transformations of a solid solution are based on two processes: (1) diffusional and (2) diffusionless; depending on the composition of the solid solution (type and concentration of the stabilizing oxide) and preparation conditions, these processes can occur either in pure form or in various combinations.

(1) The mechanism of the diffusion process involves decay of the solid solution according to the phase diagram. In this case, nucleation sites of the tetragonal phase are formed in the bulk of the original cubic solid solution; these nucleation sites are depleted of the stabilizing oxide in comparison with the original composition (phase *t*). Accordingly, the cubic matrix is enriched in the stabilizer and undergoes transition to the tetragonal phase at lower temperatures to give the so-called phase *t′*. At temperatures of about 1000–1200 °C, diffusion is hindered and this type of mechanism is disabled.

(2) Formation of the tetragonal phase at temperatures below 1200 °C results in the formation of domains of this phase by the diffusionless mechanism. The chemical composition of the resulting domains is similar to that of the original cubic phase. Detailed data on the mechanism of phase transformations in PSZ are provided in ref. 1.

Thus, an interpretation of phase transformations involved in the formation of PSZ crystals is a multi-parameter task that requires further efforts.

The actual structure of PSZ crystals has been studied in detail.[22,23] The studies have been carried out by X-ray diffraction, Raman scattering, SEM and transmission electron microscopy (including high resolution methods).

Table 4 presents data on the studies of PSZ with various compositions using the ‘rocking curves’ method on a two-crystal X-ray diffractometer. The sizes of coherent scattering areas were determined from broadening of the (111) and (222) diffraction maxima. One can see from the data in the table that the crystals have a nanodomain structure. The sizes of the domains depend on the composition, growth mode and subsequent thermal treatment. A study of PSZ microstructure by SEM and optical

Table 4 Nanostructure of PSZ crystals determined by X-ray diffraction (rocking curve method).

Composition, mol.%			Post-growth annealing	Growth direction	D^a/nm	α^b/°
ZrO_2	Y_2O_3	CeO_2				
97	3	—		331	6.7	1–2
96.4	3.5	0.1	1200 °C, vacuum 10^{-4} Torr, 2 h	111	8.1	2–8
97.3	2.5	0.2	1200 °C, vacuum 10^{-4} Torr, 2 h	111	20	2–8
97.3	2.5	0.2	1200 °C, vacuum 10^{-4} Torr, 6 h	111	26	1–2
97.3	2.5	0.2	2200 °C, vacuum 10^{-4} Torr, 2 h	111	50	1–2

[a]*D* is the size of coherent scattering areas, nm. [b]α is the domain's mean disordering angle, deg.

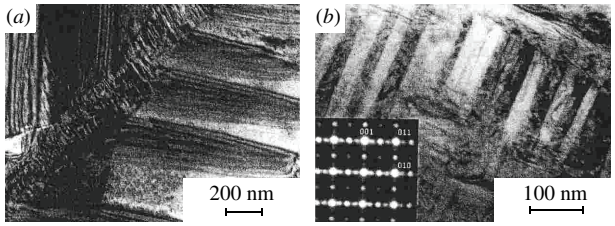

Figure 4 Electron microscope images of PSZ samples. (*a*) ZrO_2–2.5 mol% Y_2O_3; growth rate, 10 mm h^{-1}. (*b*) ZrO_2–3.0 mol% Y_2O_3; growth rate, 10 mm h^{-1}. Inset: electron diffractogram.

microscopy showed that it has a multilevel hierarchy. The nanostructure of PSZ can be revealed in a most illustrative and informative way using high-resolution transmission electron microscopy (Figure 4).

The nanostructure of PSZs with various compositions was studied using JEM 2100 (Jeol) and EM 430ST (Philips) high-resolution transmission electron microscopes.

The starting samples of ZrO_2–3 mol% Y_2O_3 had the form of plates 200 μm thick. Discs 3 mm in diameter were ultrasonically cut from the plate. Further, a cavity with a bottom thickness of 20 μm was ground in a disc. The layer at the cavity bottom disturbed due to mechanical treatment was removed by ion etching.

Figure 4 shows some most typical electron microscopic images. Analysis of electron microscopic images confirmed that a cubic–tetragonal phase transformation occurs during cooling of crystals grown in the ZrO_2–Y_2O_3 system in the concentration range of 2.5–4 mol% Y_2O_3. As a result, a hierarchical micro- and nanostructure is formed, including ordered zones with parquet-like packing or stacks of plates resembling mica. The size of first-level domains is about 10 nm. Ordered zones alternate with zones built of randomly arranged nanodomains of various

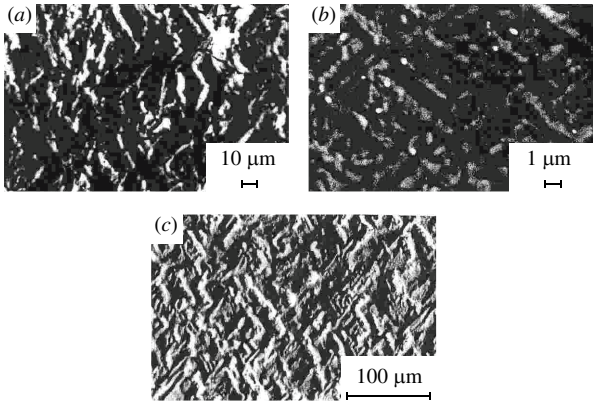

Figure 5 Microstructure of non-treated (as-grown) surface of PSZ crystals. (*a*) ZrO_2–2.0 mol% Y_2O_3. (*b*) ZrO_2–2.5 mol% Y_2O_3. (*c*) ZrO_2–3.0 mol% Y_2O_3. The crystal growth rate was 10 mm h^{-1} in all cases.

shapes, such as prisms, plates or needles. Comparison of results obtained using various techniques made it possible to establish the relationship between the nano- and microstructure of PSZ and the structure of its surface. Figure 5 demonstrates the micrographs of the surface of PSZ crystals obtained under the same conditions but differing in composition. One can see that, as the concentration of Y_2O_3 increases, the weakly ordered microstructure penetrated by cracks is gradually converted to an ordered tweed structure without violation of continuity. The surface structure well correlates with the three-dimensional nanostructure. Thus, the surface pattern on PSZ crystals is a good diagnostic indicator of the 3D nanostructure.

Properties of PSZ crystals. The unique nanodomain structure of PSZ provides a combination of properties that differ both from those of single-crystal phianites and from sintered ceramics with the corresponding composition (Table 5). First, note that the specific density of PSZ is the maximum possible value for this composition, which results from the conservation of continuity and complete absence of porosity. In this respect, PSZ is most similar to single-crystal phianites and is superior to sintered ceramics. On the other hand, PSZ significantly exceeds phianites in other structure-sensitive properties, such as strength properties. PSZ is especially superior in such property as fracture strength, which is characterized by dynamic stress intensity factor K_{1c}. With respect to this parameter, PSZ exceeds other nonmetallic materials as well (see Table 5). The high strength of PSZ goes together with remarkable tribotechnical characteristics: very low friction factor and especially high wear resistance. In addition, PSZ maintains excellent mechanical properties over a broad temperature range (–140 to 1400 °C), as

Table 5 Comparative characteristics of non-metal structural materials.

Properties	PSZ crystals	PSZ ceramics	Phianite crystals	α-Al_2O_3 (corundum) crystals	Silicon carbide	Silicon nitride ceramics
Chemical composition	ZrO_2–Y_2O_3	ZrO_2–Y_2O_3	ZrO_2–Y_2O_3	α-Al_2O_3	SiC	SiN
Specific density	6080	~ 6000	5870	3960	3220	3440
Melting point/°C	2780	2780	2805	2050	—	—
Thermal expansion coefficient β; deg^{-1} (at 200 °C)	(10–11)×10^{-6}	10.2×10^{-6}	10.5×10^{-6}	8×10^{-6}	4.2×10^{-6}	3.2×10^{-6}
Microhardness, *H*/GPa	11.8–15.8	12.8	14.55	15.4	24–29	14
Flexural strength, σ_m/ MPa	800–1200	696–980	224	214	500–600	600–900
Compressive strength, σ_m, MPa	2300–3700	1900	1760	—	3500	—
Dynamic modulus of elasticity, *E*/GPa	180–372	300	210	—	380	—
Poisson number, μ_0	0.26–0.36	—	0.30	—	—	—
Fracture strength, *K*1c/MPa $m^{1/2}$	6–12	5.8–9.0	—	3–4	3–4	5–7
Friction factor, f [a]	0.12–0.34	—	0.21	0.5	—	0.4
Wear intensity, J[a]	(0.17–3)×10^{-9}	—	2.73×10^{-8}	—	—	—

[a]The tribotechnical characteristics *f* and *J* correspond to the following testing mode: P = 5 MPa, v = 2 m s^{-1}, without lubrication; wear intensity $J = h/L$, where h is the thickness of the worn-out layer; L is the slip distance.

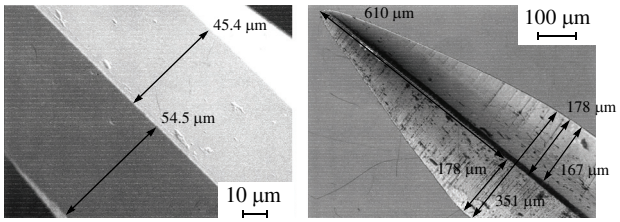

Figure 6 Electron microscope images of edges of surgical scalpels. (*a*) PSZ; (*b*) special alloy.

Figure 7 Scalpels for cardio- and neurosurgery, maxillofacial and embryo surgery, cosmetic and ophthalmologic operations.

well as chemical inertness and biological compatibility. These properties are not structure dependent; however, combined with the above mechanical and tribotechnical characteristics, they make PSZ crystals attractive for many technical and medical applications.

The most promising applications of materials based on PSZ crystals. Currently, the most advanced use of PSZ is to make cutting tools, especially medical scalpels. The use of PSZ in this area is based on the fact that the cutting edge can be honed to extreme sharpness and is resistant against rupture during surgery. It is also important that the low friction factor of the material and its biocompatibility make it possible to avoid damage to biotissue. Figure 6 shows electron micrographs of scalpel edges made of PSZ and of special steel. The advantages of PSZ scalpels are evident: ultimate sharpness (as thin as 100 nm) and high edge uniformity. Figure 7 shows pictures of various scalpels, *i.e.*, for cardio- and neurosurgery, maxillofacial and embryo surgery, cosmetology and ophthalmology.

The resistance of PSZ against abrasive wear allows it to be used in dies and extruders for wire-drawing, in the production of glass and basalt fiber, in rolls for finest bands and foils, and in milling bodies for ball mills. Figure 8 shows a draw plate with a profiled PSZ die for producing aluminum and copper wire.

The high tribotechnical characteristics allow PSZ crystals to be used in parts of friction couples: pistons, cylinder sleeves, valves and valve seats for extremely drastic conditions, gate valves for gas- and oil-extracting industries, thread guides and slide bars in textile manufacturing machines, parts of dry bearings and ball bearings.

Figure 8 Photograph of a draw plate with profiled PSZ die for producing aluminum and copper wire.

A special place belongs to the quickly-developing application of PSZ crystals in bioinert implants with high fatigue strength for dental and orthopedic surgery.

In conclusion, note that the structure of PSZ is extremely flexible. It depends in a complex way on the composition (in particular, type and concentration of the second and third components of the solid solution), as well as on the thermal conditions during the formation and additional thermal treatment. Strictly speaking, a whole range of materials characterized by various particular combinations of structure-sensitive properties is in question. In turn, this fact makes it possible to optimize the material properties for specific practical applications. On the other hand, this kind of 'fine tuning' requires additional studies. In particular, it is very important to reveal the relationship between the processes of cubic-to-tetragonal polymorphic transformation, on the one hand, and those of diffusion decay of the solid solution, on the other. The latter process results in the formation of domains with various chemical compositions, which allows us to consider PSZ crystals as not only nanostructured but also composite materials.

This work was partially supported by ISTC (contract no. 2242), Programme of Presidium of the Russian Academy of Sciences 'Support for innovation and development' no. 04-068, Russian Foundation for Basic Research (grant no. 06-08-00014) and State contract no. 02.523.1.3018.

The author is sincerely grateful to L. M. Ershova for her assistance in preparing the text and to E. V. Chernova for her assistance in preparing the figures.

References

1 Yu. S. Kuz'minov, E. E. Lomonova and V. V. Osiko, *Tugoplavkie materialy iz kholodnogo tiglya* (*Refractory Materials from Cold Crucible*), Nauka, Moscow, 2004 (in Russian).
2 Yu. S. Kuz'minov, E. E. Lomonova and V. V. Osiko, *Cubic Zirconia and Skull Melting*, Cambridge International Science Publishing, UK, 2008.
3 Yu. S. Kuz'minov, E. E. Lomonova and V. V. Osiko, *Refractory Materials from Cold Crucible*, 2006 (in Chinese).
4 J. Lu, R. Ueda, H. Yagi, T. Yanagitani, Y. Akiyama and A. Kaminskii, *J. Alloys Compd.*, 2002, **341**, 220.
5 T. T. Basiev, M. E. Doroshenko, V. A. Konyushkin, V. V. Osiko, P. P. Fedorov, V. A. Demidenko, K. V. Dukel'skii, I. A. Mirov and A. N. Smirnov, *Izv. Akad. Nauk, Ser. Khim.*, 2008, 863 (*Russ. Chem. Bull., Int. Ed.*, 2008, **57**, 877).
6 T. T. Basiev, V. V. Voronov, V. A. Konyushkin, S. V. Kuznetsov, S. V. Lavrishchev, V. V. Osiko, P. P. Fedorov, A. B. Ankudinov and M. I. Alymov, *Dokl. Akad. Nauk*, 2007, **417**, 631 (in Russian).
7 G. B. Kurdyumov, *Nesovershenstva kristallicheskogo stroeniya i material'nye prevrashcheniya. Sbornik statei* (*Crystal Structure Defects and Material Transformations. Collection of papers*), Nauka, Moscow, 1972 (in Russian).
8 Yu. S. Kuz'minov and V. V. Osiko, *Fianity* (*Phianites*), Nauka, Moscow, 2001 (in Russian).
9 H. G. Scott, *J. Mater. Sci.*, 1977, **12**, 311.
10 V. I. Aleksandrov, V. V. Osiko and V. M. Tatarintsev, *Pribory i Tekhnika Eksperimenta*, 1970, no. 5, 222 (in Russian).
11 V. I. Aleksandrov, V. V. Osiko, A. M. Prokhorov and V. M. Tatarintsev, *Izv. Akad. Nauk SSSR, Ser. Inorg. Mater.*, 1972, 956 (in Russian).
12 V. I. Aleksandrov, V. V. Osiko, A. M. Prokhorov and V. M. Tatarintsev, *Vestnik Akad. Nauk SSSR*, 1973, **312**, 29 (in Russian).
13 V. I. Aleksandrov, V. V. Osiko, A. M. Prokhorov and V. M. Tatarintsev, in *Current Topics in Materials Science*, ed. E. Kaldis, North-Holland, Amsterdam, 1978, vol. 1, pp. 421–480.
14 V. I. Aleksandrov, V. V. Osiko, A. M. Prokhorov and V. M. Tatarintsev, *Usp. Khim.*, 1978, **47**, 385 (*Russ. Chem. Rev.*, 1978, **47**, 213).

15 M. A. Borik, E. E. Lomonova, V. V. Osiko and A. M. Prokhorov, *Problemy kristallografii* (*Problems of Crystallography*), ed. B. K. Vainstein, Nauka, Moscow, 1987, pp. 165–189 (in Russian).
16 V. V. Osiko and J. F. Wenckus, in *Book of Lecture Notes. First International School on Crystal Growth Technology*, Beatenberg, Switzerland, 1998, pp. 580–591.
17 Yu. K. Voron'ko, M. A. Zufarov, B. V. Ignat'ev, V. V. Osiko, E. E. Lomonova and A. A. Sobol, *Opt. Spectrosk.*, 1981, **51**, 569 (in Russian).
18 A. A. Sobol and Yu. K. Voron'ko, *J. Phys. Chem. Solids*, 2004, **65**, 1103.
19 N. Yoshikawa and H. Sato, *J. Jpn. Inst. Met.*, 1986, **50**, 108.
20 A. G. Khachaturyan, *Teoriya fazovykh prevrashchenii i struktura tverdykh rastvorov* (*Theory of Phase Transformations and Structure of Solid Solutions*), Nauka, Moscow, 1974, p. 383 (in Russian).
21 T. Mitsuhashi, *J. Am. Ceram. Soc*., 1973, **48**, 493.
22 M. Anglada, G. Alkala, R. Fernandez, L. Llanes and D. Casellas, *Proceedings of the 7th International Symposium on the Fracture Mechanics of Ceramics*, Moscow, 1999; in *Fracture Mechanics of Ceramics*, eds. R. C. Bradt and D. Munz, Kluwer, 2002, vol. 13, p. 255.
23 J. Chevalier, L. Gremillard, R. Zenati, Y. Jorand, C. Olagnon and G. Fantozzi, *Proceedings of the 7th International Symposium on the Fracture Mechanics of Ceramics*, Moscow, 1999; in *Fracture Mechanics of Ceramics*, eds. R. C. Bradt and D. Munz, Kluwer, 2002, vol. 13, p. 287.
24 M. A. Borik, Yu. K. Voronko, E. E. Lomonova, V. V. Osiko, V. A. Sarin and G. A. Gogotsi, *Proceedings of the 7th International Symposium on the Fracture Mechanics of Ceramics*, Moscow, 1999; in *Fracture Mechanics of Ceramics*, eds. R. C. Bradt and D. Munz, Kluwer, 2002, vol. 13, p. 485.
25 M. A. Borik, M. A. Vishnyakova, O. M. Zhigalina, A. V. Kulebyakin, S. V. Lavrishchev, E. E. Lomonova and V. V. Osiko, *Ross. Nanotekhnol.*, 2008, **3** (11–12), 76 (in Russian).

Received: 30th January 2009; Com. 09/3278